



Spatial and Temporal Variability in Water Quality and Phytoplankton Community Composition in Charleston Harbor

ABIGAIL STEPHENS¹, NICOLE SCHANKE¹, EMMALINE SHEAHAN^{1,2}, AND GIACOMO DiTULLIO¹

AUTHORS: ¹Grice and Hollings Marine Laboratories, College of Charleston, 205 Fort Johnson Road, Charleston, SC, 29412, USA.

²Florida Museum of Natural History, University of Florida, Gainesville, FL 32611, USA.

Abstract. The Charleston Harbor estuary is a dynamic ecosystem draining three rivers that surround the rapidly urbanizing greater Charleston area. Projected climate change impacts include elevated sea surface temperature and local changes in water quality that will likely alter biogeochemical cycling as well as phytoplankton abundance and community composition. Partnering with the local non-profit organization *Charleston Waterkeeper*, surface water samples were collected from late April through October 2021 at 20 sites in the Charleston Harbor estuary system. Water quality parameters measured included sea surface temperature (SST), salinity, pH, dissolved inorganic carbon, chromophoric dissolved organic matter (CDOM), phytoplankton pigments and nitrate and phosphate concentrations. Relatively high (6–16 μM) nitrate values were observed throughout the year and the nitrate to phosphate (N:P) ratios were consistently elevated (50–200) relative to the Redfield ratio of 16. Analysis of variance indicated that the delivery of nitrate, phosphate, and CDOM into the estuary came from upriver of the Charleston Harbor. For instance, CDOM was significantly impacted by tidal stage ($p < 0.05$) and was negatively correlated with salinity at low salinity sites, but no correlation was observed at high salinity sites. Seasonal patterns in phytoplankton community abundance and composition were driven by changes in SST, as overall phytoplankton biomass increased with a community shift from diatoms during colder months to flagellated cells such as prasinophytes during the warmer summer months. Phytoplankton diversity was greatest during the early summer and lowest in October. This study provides a reference baseline for water quality parameters and phytoplankton community composition in an estuarine ecosystem that is changing rapidly due to dredging and climate change processes.

INTRODUCTION

Estuaries are dynamic coastal ecosystems found at the land-sea interface. These ecosystems are greatly influenced by inputs of freshwater from rivers, saltwater from the ocean, and daily tidal mixing. Typically, freshwater from upriver brings macronutrients and sediments to the estuary as a result of surface and stormwater runoff (Pinckney et al. 1997; Statham 2012; Reed et al. 2016; Chin et al. 2022). This nutrient loading not only supports primary production in estuaries but can also result in eutrophication when an overabundance of nutrients is available (Lee et al. 2006; Statham 2012; Reed et al. 2016; Freeman et al. 2019). One of the key contributors to excessive nutrient input into estuaries is urban development, which is rapidly increasing in coastal areas (Lee et al. 2006; Freeman et al. 2019). The urbanization of natural ecosystems and the increase in impervious surface cover prevent runoff filtration through the soil and thereby introduces elevated amounts of pollutants, sediments, and

nutrients to estuaries (Lee et al. 2006; Reed et al. 2016). While estuaries are naturally dynamic ecosystems, they are also vulnerable to significant anthropogenic influences.

Urbanization and changes in land use and land cover alter river drainage patterns and subsequently the delivery of organic matter and macronutrients (i.e., nitrogen (N) and phosphorus (P)) to coastal ecosystems (Paerl et al. 2007; Rothenberger et al. 2009). Not only can an increase in stormwater runoff from land result in elevated concentrations of nitrogen and phosphorus, but it can also change the relative elemental composition of these nutrients (i.e., the N:P ratio) in local waters. The imbalance between N and P fluxes to salt marsh estuaries has led to an anthropogenic-driven increase in the N:P ratio with respect to the Redfield N:P ratio of 16 (Redfield 1934; McDowell et al. 1995). In these ecosystems, urbanization is increasing the N input as impervious surface cover reduces the ability of riparian zones to serve as N sinks, and greater volumes of sewage and wastewater discharge are becoming more significant N sources (Groffman et al. 2002;

Glibert et al. 2006; Reed et al. 2016). However, the input of P is decreasing due to the high tendency of P to adsorb to soil particles and the recent bans on P in detergents (Schlesinger and Bernhardt 2013). Therefore, increased urbanization may significantly impact the relative composition of macronutrient delivery into estuaries and coastal waters, which could have important implications for phytoplankton community composition.

Estuaries support taxonomically diverse phytoplankton communities because of the interactions between human-impacted freshwater input and oceanic saltwater influxes (Cloern and Jassby 2008; Carstensen et al. 2015). In these ecosystems, phytoplankton communities are often dominated by diatoms and dinoflagellates, with smaller contributions from chlorophytes and cyanobacteria (Pinckney et al. 1998; Richardson et al., 2010; Reed et al. 2016; Carstensen et al. 2015; Allen et al. 2016). However, changes in phytoplankton abundance and community composition can be influenced by seasonal changes in temperature, episodic nutrient inputs from rivers (especially following heavy rain events), changes in nutrient stoichiometry (i.e., N:P ratios), salinity gradients, and tidal mixing (Mallin et al. 1991; Pinckney et al. 1998; Cloern and Jassby 2008; Carstensen et al. 2015). For example, diatoms thrive in turbulent waters and under high nutrient conditions which allows this algal group to dominate estuaries, especially in the spring as nutrient levels are typically elevated (Mallin et al. 1991; Carstensen et al. 2015). Nitrogen-fixing cyanobacteria often form blooms in lower salinity waters during the summer when sea surface temperatures (SSTs) are high and nitrate has been relatively depleted (Pinckney et al. 1997; Paerl and Huisman 2009; Rothenberger et al. 2009; Carstensen et al. 2015). There is evidence that chlorophytes also may be better adapted to lower salinity waters than to brackish estuaries (Carstensen et al. 2015). Summer and autumn blooms of diatoms, dinoflagellates, and other flagellated species have been observed as well (Mallin et al. 1991; Carstensen et al. 2015). Seasonal and spatial patterns in phytoplankton community composition and bloom dynamics are difficult to predict given the highly variable physical and chemical (i.e., nutrient) conditions within a single estuary and the even greater variety in hydrodynamic features between estuaries (Cloern and Jassby 2008; Carstensen et al. 2015).

While challenging, understanding estuarine phytoplankton communities is important as species composition can influence carbon sequestering, biogeochemical cycling, food web dynamics, fisheries, and human health (Mallin et al. 1991; Carstensen et al. 2015). Of particular interest in this study is the potential for growth of harmful algal bloom (HAB) species. While eutrophication can stimulate the rapid growth of most, if not all, phytoplankton species, special concern is given to noxious or toxic algae (Rothenberger et al. 2009). These HAB-forming phytoplankton species can pro-

duce and release toxins, having direct impacts on water quality and ecosystem health. HAB species that do not produce toxins can still detrimentally affect the ecosystem as the large quantity of biomass eventually decays and drives a biochemical oxygen demand (Anderson et al. 2002; Riekenberg et al. 2015). Estuarine species from a variety of phytoplankton groups have the ability to produce and release toxins, which can impact the health of these communities and the human populations near these waters. For example, species of estuarine diatoms (e.g., *Pseudo-nitzschia* spp.; Fernandes et al. 2014), dinoflagellates (e.g., *Karenia* spp. and *Alexandrium* spp.; Verma et al. 2019), raphidophytes (*Heterosigma* spp. and *Chatonella* spp.; Rothenberger et al. 2009) and cyanobacteria (e.g., *Anabaena* spp. and *Microcystis* spp.; Carmichael 2012) have shown evidence of toxin-production. Having a greater understanding of estuarine phytoplankton communities and how they are likely to be altered by changes in water quality, specifically in ecosystems impacted by increasing urbanization and fluctuating nutrient conditions, will help evaluate the potential threat of HABs on overall ecosystem health.

The Charleston Harbor is a coastal plain estuary located on the southeastern coast of South Carolina, and receives freshwater inputs from the Ashely, Cooper, and Wando Rivers (Dustan and Pinckney 1989). The Ashley and Wando Rivers contain extensive tidal creeks that contribute little freshwater, while the Cooper River supplies most of the freshwater to the Charleston Harbor, at rates of $110170 \text{ m}^3 \text{ s}^{-1}$ (Dustan and Pinckney 1989; Yassuda et al. 2000). While most of the land surrounding the Charleston Harbor estuary is highly developed, especially to the north and upriver of the harbor, there are smaller forested areas to the southwest of the harbor and an extensive system of tidal creeks and wetlands along the coast (Figure 1; Fry et al. 2011). Charleston Harbor is also being greatly impacted by urbanization. From 1995–2015, Charleston County had an urban expansion rate of 26.7% and during that time over 32 km^2 of coastal areas were developed as “newly urbanized lands” (Xu and Liu 2022). Concomitant with its low elevation, urbanization is exacerbating the degree of nuisance flooding in Charleston. In 1988, it was estimated that nuisance flood conditions on the Charleston peninsula occurred on fewer than ten days, yet in 2014 this grew to 25 flood days, and by 2051 models predict nuisance flood conditions will occur on 60 days during the year (Morris and Renken 2020). With these unprecedented rates of urbanization in an area already vulnerable to flooding, it is expected that the Charleston Harbor estuary and the surrounding coastal ecosystems will be greatly impacted by elevated levels of surface and stormwater runoff that are likely to alter local water quality.

The present study was conducted to investigate how short-term (April to October 2021) spatial and temporal variability in water quality conditions could impact the phytoplankton community composition in the Charleston

Harbor estuary. The sampling area consisted of 20 sites covering approximately 80 mi² of the greater Charleston area and included sites near more urbanized, populated areas further upriver as well as less developed, more pristine areas closer to the coast. Because of the spatial scale of this study, comparisons of water quality and phytoplankton communities were made between the relatively more urbanized, upriver sites and the relatively less developed, coastal sites. It was hypothesized that as water temperatures increased in the summer the phytoplankton community would shift from diatoms towards cyanobacteria or other picoplankton, with an increase in overall phytoplankton biomass. It was also expected that the more urbanized, upriver sites would have lower salinities, higher nutrient levels and higher relative chromophoric dissolved organic matter (CDOM) levels than the less developed, more coastal sites. While similar studies have been conducted in other southeast Atlantic estuaries (e.g., North Inlet, SC, Savannah River, GA and St. Johns River, FL; Tufford et al, 2003; Bittar et al. 2016; Dame et al. 2000; Van Meerssche and Pinckney 2018; Pinckney et al. 2020; Wang and Zhang 2020), there is a scarcity of water quality surveys in the Charleston Harbor estuary. It is essential to form a baseline understanding of this estuary system to better predict changes in water quality in the coming decades that will be important for informing future management resource decisions.

MATERIALS AND METHODS

SEAWATER COLLECTION

Seawater samples were collected at 20 sites within the greater Charleston Harbor area in conjunction with the non-profit, citizen science group, *Charleston Waterkeeper* (Figure 1, Table 1). Surface seawater was collected weekly from April 28, 2021, to October 27, 2021. Due to technical issues, no samples were collected on May 12, and only 14 and 16 of the 20 samples were collected on July 28 and August 18, respectively. Due to boat ramp closures, samples were not collected from the SR1 site from June 9–June 30. Samples were collected from each site in the same order every week with collection times typically occurring within a 4-hour window in the morning. Because of this, the tidal stage at which samples were collected varied from week to week.

Surface seawater samples from each site were collected in acid-clean, 500 mL opaque, amber polyethylene bottles and returned to the lab for processing within 36 hours after collection. SST, total chlorophyll *a* (TChl_a), and accessory pigment concentrations were measured throughout the entire sampling period, while salinity measurements started on June 16 and nutrient and carbon measurements started on Jul 7. Rainfall data was collected from the National Weather Service's NOWData database (<https://www.weather.gov/wrh/Climate?wfo=chs>). Average 7day cumulative rainfalls

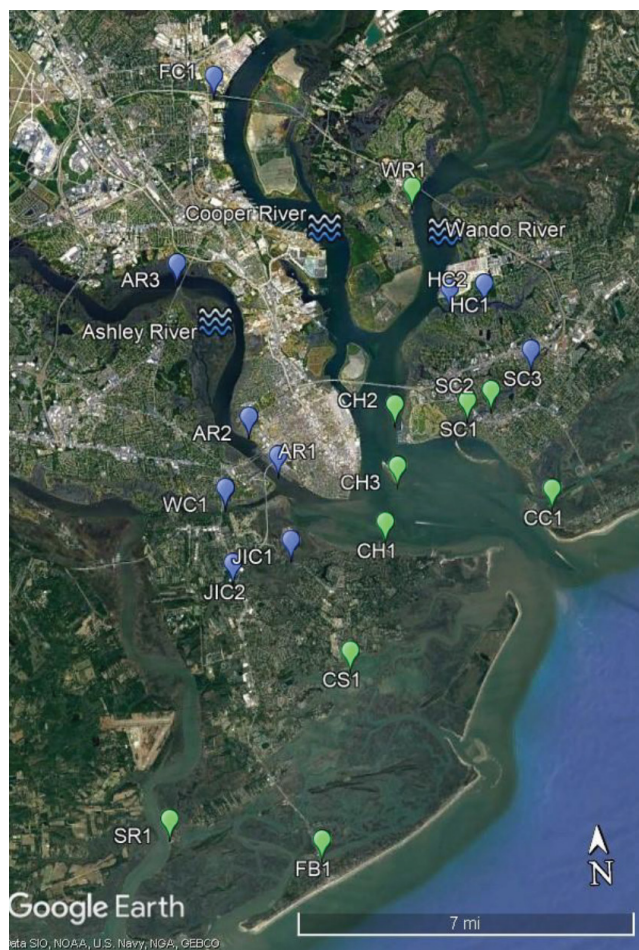


Figure 1. Map of sampling sites within the greater Charleston Harbor area. Site names and coordinates are found in Table 1. Low salinity sites (LSS) are designated by a blue marker and high salinity sites (HSS) are designated by a green marker.

were taken from 13 weather stations across the sampling area. The tidal heights at which each sample was collected were determined by NOAA's Tides and Currents database (https://tidesandcurrents.noaa.gov/tide_predictions.html). Each of the 20 sampling sites was matched with the closest NOAA station for which tidal data was provided. Within the greater Charleston Harbor area, NOAA designated the Charleston Custom House Wharf station (station 8665530) as the "reference station." This allowed the tidal height at the reference station to be adjusted to each of the 20 sampling sites by multiplying the reference station tidal height by the "tidal height offset" recorded in Table 1.

To make comparisons between the upriver and coastal locations, the 20 sampling sites were divided into two groups based upon each site's average salinity across the sampling season. Sites with average salinities below the overall average salinity were defined as "low salinity sites" and represented the locations further upriver, while sites with average salinities above the overall average salinity were defined as "high

Spatial and Temporal Variability in Water Quality and Phytoplankton Community Composition

Table 1. Summary of site names and locations. Tidal height offset is the factor multiplied by the tidal height (in feet) at the Reference Station to calculate the adjusted tidal height at each site, during both high and low tides. Calculations for % impervious surface cover and salinity grouping (low salinity site “LSS” or high salinity site “HSS”) are described in the methods and results.

Site Name	Site Location	Tidal Height Offset	% Impervious Surface Cover	Salinity Grouping
Ashley River 1 (AR1)	32°46'34.62" N -79°57'12.42" W	High: 1.01 Low: 1.05	36.5	LSS
Brittlebank Park (AR2)	32°47'17.92" N -79°57'48.02" W	High: 1.01 Low: 1.05	26.2	LSS
Northbridge Park (AR3)	32°50'6.98" N -79°59'12.49" W	High: 1.07 Low: 1.05	8.77	LSS
Cove Creek 1 (CC1)	32°45'45.95" N -79°51'22.23" W	High: 0.97 Low: 0.95	9.70	HSS
Melton Peter Demeter Park (CH1)	32°45'17.93" N -79°54'58.04" W	High: 0.97 Low: 1	9.80	HSS
CofC Sailing (CH2)	32°47'24.30" N -79°54'39.60" W	Reference Station	16.4	HSS
Battery Beach (CH3)	32°46'17.82" N -79°54'39.60" W	Reference Station	56.9	HSS
Clark Sound (CS1)	32°43'0.18" N -79°55'50.03" W	High: 1.04 Low: 1	5.14	HSS
Folly Beach Boat Landing (FB1)	32°39'37.21" N -79°56'36.64" W	High: 1.01 Low: 0.95	17.0	HSS
Filbin Creek 1 (FC1)	32°53'28.45" N -79°58'15.21" W	High: 1.03 Low: 1	41.8	LSS
Hobcaw Creek 1 (HC1)	32°49'27.37" N -79°53'22.89" W	High: 1.03 Low: 0.95	25.2	LSS
Hobcaw Creek 2 (HC2)	32°49'30.88" N -79°52'38.23" W	High: 1.03 Low: 0.95	20.8	LSS
James Island Creek 1 (JIC1)	32°45'2.51" N -79°57'0.48" W	High: 1.02 Low: 1.05	5.54	LSS
James Island Creek 2 (JIC2)	32°44'40.20" N -79°58'16.20" W	High: 1.02 Low: 1.05	18.9	LSS
Shem Creek Park Dock (SC1)	32°47'25.50" N -79°53'6.23" W	High: 0.99 Low: 1	19.7	HSS
Shem Creek Public Boat Land- ing (SC2)	32°47'35.50" N -79°52'35.27" W	High: 0.99 Low: 1	24.3	HSS
Shem Creek 3 (SC3)	32°48'17.34" N -79°51'41.75" W	High: 0.99 Low: 1	25.1	LSS
Stono River 1 (SR1)	32°40'6.17" N -79°59'51.01" W	High: 1.01 Low: 0.95	0.66	HSS
Wappoo Cut Boat Ramp (WC1)	32°46'1.75" N -79°58'21.86" W	High: 0.99 Low: 0.99	17.3	LSS
Wando River (WR1)	32°51'19.36" N -79°54'5.73" W	High: 1.03 Low: 0.95	28.5	HSS

salinity sites” and represented the locations closer to the coast.

IMPERVIOUS SURFACE COVER

The percentage of impervious cover (Table 1) was calculated using data from the Land Cover Basin Characteristics Rasters for South Carolina StreamStats 2021 (Gurley and Kolb 2021). A 0.01 degree (approximately 0.7 mi) circular buffer was drawn around each sampling site and the average percent impervious cover for the land within that buffer was reported. The code written to output these statistics can be accessed at https://github.com/EmmalineSheahan/chas_water_keeper.

NUTRIENT MEASUREMENTS

Sample aliquots were filtered through GF/F (Whatman) filters into 50 mL sterile conical tubes and frozen at -20° until analysis (less than six months). Nitrate and phosphate concentrations were measured using standard spectrophotometric analyses (Parsons et al. 1984). Nitrate analysis used 2% resorcinol and sulfuric acid while phosphate analysis used a mixed reagent containing ammonium molybdate, sulfuric acid, ascorbic acid, and potassium antimonyl tartrate to produce the colorimetric reactions. Absorbance was measured on a dual beam spectrophotometer (Shimadzu UV1601, Tokyo, Japan) at 505 nm for nitrate analysis and 885 nm for phosphate analysis. Standard curves ranged from 0-400 μM and 0-1 μM for nitrate and phosphate analyses, respectively, and all samples fell within this range of concentrations. Standards and appropriate blanks were made using Milli-Q water (resistivity > 18 m Ω).

CARBON PARAMETERS

Sample aliquots of 50 mL were filtered through combusted (at 450°C for 45 hours) GF/F (Whatman) filters, using acid-clean glassware. The filtrate was collected into acid-clean 60 mL polyethylene bottles and frozen at -20°C until subsequent processing. CDOM measurements were performed on a dual beam spectrophotometer (Shimadzu UV1601, Tokyo, Japan). Action spectra on the filtrate samples were collected from 350 to 700 nm using a 5 cm quartz cuvette. The absorbance at 412 nm served as a proxy for relative CDOM (Danhez et al. 2017). As in other studies, CDOM was used as a proxy for dissolved organic carbon (DOC) concentrations. Carbonate alkalinity was measured colorimetrically using the bromophenol blue method (Sarazin et al. 1999), with absorbance measurements made at 590 nm in a 1 cm quartz cuvette. pH was measured using a Symphony SB20 pH meter (VWR Scientific Products, Radnor, PA, USA), calibrated at pH values of 4, 7, and 10.

PHYTOPLANKTON BIOMASS

Sample aliquots of 200 mL were filtered onto 25 mm GF/F (Whatman) filters and frozen at -80°C until processed using high performance liquid chromatography (HPLC) methods. Photosynthetic pigments were extracted in 1390 μL of HPLC-grade acetone and 10 μL trans- β -Apo-8'-carotenal(internal standard) at -20°C for 24 hours. Pigment extracts (600 μL) were 0.2 μm syringe-filtered and analyzed on an Agilent 1100 Series HPLC using diode array and fluorescence detectors (Agilent Technologies, Santa Clara, California). A Waters Symmetry C8 column (4.6x150 mm, 3.5 μm packing size) was used with binary mobile phases of methanol:acetonitrile:0.25 M pyridine (50:25:25 v:v:v) and methanol:acetonitrile:acetone (20:60:20 v:v:v; DiTullio and Geesey 2003). Agilent's ChemStation software (version B.03.03) was used to calculate pigment concentrations from integrated areas on the resulting HPLC chromatograms. Pigment concentrations were calibrated using pure algal cultures and pigment standards from DHI (Copenhagen, Denmark). Detection limits were approximately 1 ng and the coefficient of variance for replicate injections was approximately 2%. TChla served as a proxy for total phytoplankton biomass and was calculated as the sum of the concentrations of chlorophyll *a*, divinyl chlorophyll *a*, a chlorophyll *a* isomer, and chlorophyllide *a*.

PHYTOPLANKTON COMMUNITY COMPOSITION

Phytoplankton community composition was assessed using the iterative matrixfactorization program CHEMTAX (version 1.95; Mackey et al. 1996) which calculates the relative contribution of TChla made by several major algal groups, based upon accessory pigment concentrations and an initial pigment ratio matrix. Twelve accessory pigments were used as biomarkers to define nine algal groups. The initial pigment ratio matrix was adapted from Lewitus et al. (2005), however, the final ratio matrices from trial runs suggested that the dataset had lower concentrations of fucoxanthin and higher concentrations of chlorophyll *c* than the initial Lewitus et al. (2005) ratio matrix attributed to the algal groups. Because of this, the initial ratio matrix from Lewitus et al. (2005) was slightly altered according to Kirchman et al. (2017) and Higgins et al. (2011) to reflect the algal community more accurately in this study. The initial and final CHEMTAX pigment matrices used in this study can be found in the supplementary section (Table S1). The nine algal groups included: (1) diatoms, (2) dinoflagellates (dinoflagellate type 1, containing peridinin), (3) cyanobacteria, (4) prasinophytes A (prasinophytes lacking prasinoxanthin), (5) prasinophytes B (prasinophytes containing prasinoxanthin), (6) chlorophytes, (7) haptophytes (lacking 19'-hexanoyloxyfucoxanthin), (8) raphidophytes and (9) euglenophytes (Lewitus et al. 2005). Separate CHEMTAX bins were created for each sampling

week to account for variation in environmental factors (i.e., light levels and nutrient availability).

STATISTICS

To test seasonal, spatial and tidal hypotheses, analysis of variances were conducted using the `aov()` function in the statistical software R, with a significance threshold value (α) of 0.05. Samples were grouped by seasons as defined by “spring” from April–May, “summer” from June–August, and “autumn” from September–October. Spatial groupings were set to compare relative upriver and downriver locations based on average site salinity, as defined in the results. Because samples were collected at a range of tidal stages, data were grouped into tide classes as defined by “high tide” when tidal heights were greater than 4 ft, “mid tide” when tidal heights were 2 to 4 ft, and “low tide” when tidal heights were less than 2 ft. A principal component analysis (PCA) was conducted on 11 variables (SST, salinity, TChl a , pH, alkalinity, phosphate, nitrate, diatoms, cyanobacteria, prasinophytes B and raphidophytes) using the statistical software R and the `stats::prcomp()` function with the variables scaled and centered. The PCA only included data from July 7 through October, as complete nutrient, pH, and alkalinity data were available for these weeks. To briefly examine the influence of the tidal stage, data in the PCA were grouped by tide class as previously defined. All resulting data below are reported as average + standard deviation (SD).

RESULTS

TEMPERATURE, SALINITY AND RAINFALL

As expected, a significant seasonal trend in SST was observed across spring, summer, and autumn of 2021 ($p < 0.001$). At the beginning and end of the 2021 sampling campaign, the average (+ SD) SSTs for all sites were $23^{\circ}\text{C} + 1^{\circ}\text{C}$ (Apr 28) and $22.2^{\circ}\text{C} + 0.7^{\circ}\text{C}$ (Oct 27), respectively (Figure 2A). Average SSTs exceeded 28° during the summer months (specifically, Jun 30 to Sept 15), with the highest average SST occurring on Aug 25 at $30.5^{\circ}\text{C} + 0.5^{\circ}\text{C}$ (Figure 2A). SST did not vary greatly among sites, as the standard deviation for each week was between 0.3 – 1.4°C (Figure 2A).

No significant seasonal trend ($p = 0.70$) in salinity was observed during the sampling season. Across all sites and all weeks, the average salinity was 22.4 PSU + 6.89 PSU. The lowest and highest average salinities occurred on August 18 (19 PSU + 10 PSU) and October 20 (26 PSU + 6 PSU), respectively; however, weekly changes in salinity were greatly influenced by the tidal stage at which samples were collected. For example, on August 18, the week with the lowest average salinity, samples were collected at near ebb tide and on October 20, the week with the highest average salinity, samples were collected at near flood tide.

To address the spatial hypothesis comparing upriver sites and downriver, coastal sites, the 20 sites were divided into two groups based on their average salinity. Sites were defined as “low salinity sites” (LSS) or “high salinity sites” (HSS) depending on whether the site’s average salinity was below or above the overall average salinity of 22.4 PSU, respectively. A significant difference was observed between the salinities of the LSS and HSS (< 0.001). The sites in each salinity grouping are shown in Figure 1 and listed in Table 1. Regardless of the salinity groupings, the FC1 site had the lowest average salinity of 5 PSU + 4 PSU and was located further upriver than any of the other sites (Table 2; Figure 1). FB1 had the highest average salinity of 34 PSU + 1 PSU and was located relatively close to the open ocean with less tidal influence (i.e., low salinity standard deviation) than other sites (Table 2; Figure 1).

Throughout the sampling season, the average 7-day rainfall accumulation was 1.25 inches. The highest rainfall occurred the week prior to June 16, with a 7-day cumulative average of 4.64 inches (Figure 2A). Seven day cumulative rainfall exceeded 2 inches on June 16, 23; July 14; August 18; and September 15 and 22 and were below 0.5 inches on May 5, 19, 26; June 2, 30; July 7, September 1, 8, 29; and October 20 (Figure 2A). The lowest and highest average weekly salinities were likely impacted by rainfall, as during the week prior to the August 18 sampling (lowest average salinity) there had been 2.18 inches of rain and during the week prior to the October 20 sampling (highest average salinity) there had been no rain in the sampling area.

NUTRIENTS

Measurements of nitrate and phosphate concentrations began on July 7, which may explain why no seasonal trends in nutrient concentrations were observed ($p = 0.79$ and $p = 0.13$, respectively) as measurements in the spring and early summer were not available. Across all samples, the average nitrate and phosphate concentrations were 10 μM + 3 μM and 0.2 μM + 0.1 μM , respectively. The highest and lowest average nitrate concentrations were measured on July 28 (16 μM + 8 μM) and October 13 (6 μM + 3 μM) (Figure 2B), respectively. The highest and lowest average phosphate concentrations occurred on September 22 (0.3 μM + 0.2 μM) and Aug 11 (0.09 μM + 0.07 μM) (Figure 2B), respectively. The average N:P ratio across all samples was 91 + 43 (Figure 2B), exceeding the Redfield estimated value of 16 (Redfield, 1934). Of the 315 samples analyzed for nutrient concentrations, only nine (i.e., $< 3\%$) had N:P ratios below 16 (JIC2 on July 7, AR3 and JIC2 on July 14, FC1 on August 18, AR2, CS1 and JIC2 on September 1 and AR3 and SC3 on October 13). While the highest average N:P occurred on July 7 (193 + 244 ; Fig. 2B), there was large spatial variation as this value ranged from 15.9 at JIC2 to 990 at SR1. Similarly,

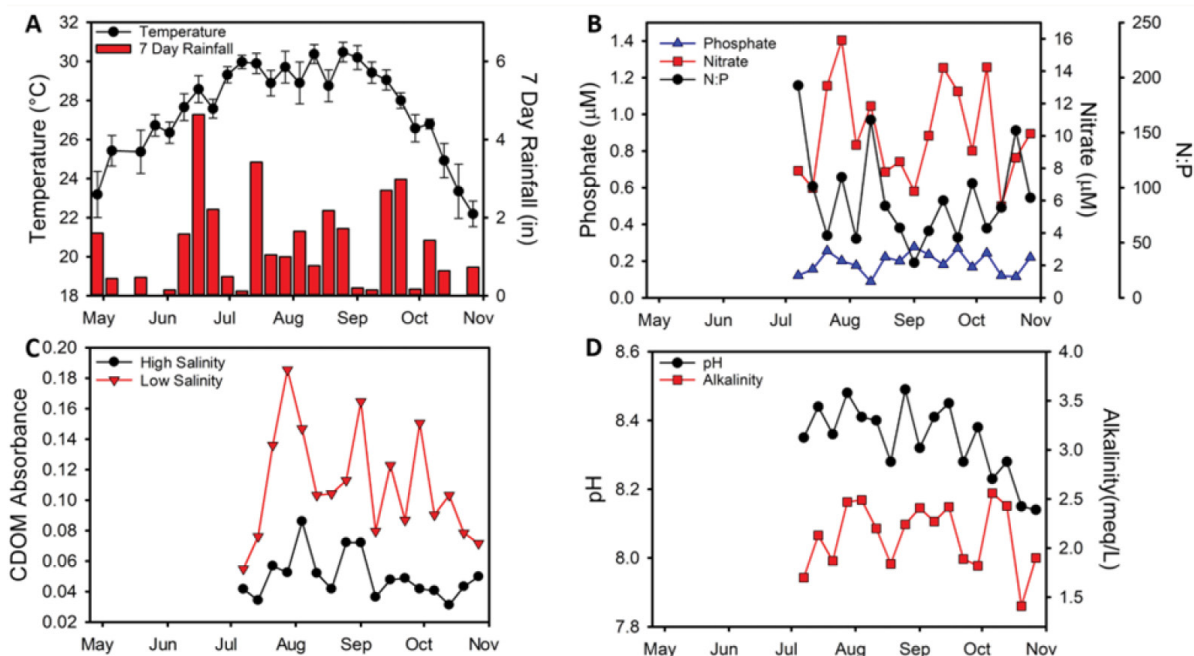


Figure 2. Water quality data during the sampling season from Apr 28 to Oct 27. Data reported are averages across all sites for each week. (A) Temperature (+ standard deviation) and cumulative rainfall from the 7 days prior to each sampling week. (B) Nitrate and phosphate concentrations (μM) and N:P ratio. (C) CDOM absorbance values at 412 nm, with data grouped into “low salinity sites” and “high salinity sites” as defined in the results and Table 1. (D) pH and carbonate alkalinity.

the lowest average N:P was $32 + 19$ on September 1, ranging from 11.4 at JIC2 and 88.3 at HC1.

The highest average nitrate and phosphate concentrations occurred at AR3 ($18 \mu\text{M} + 8 \mu\text{M}$ and $0.6 \mu\text{M} + 0.2 \mu\text{M}$, respectively), and the lowest average concentrations occurred at FB1 ($6 \mu\text{M} + 2 \mu\text{M}$ and $0.07 \mu\text{M} + 0.08 \mu\text{M}$, respectively) (Table 2). Among the sites, average N:P was the lowest at AR3 and JIC2 ($34 + 20$ and $34 + 25$, respectively), driven by relatively high average phosphate concentrations at these two locations ($0.6 \mu\text{M} + 0.2 \mu\text{M}$ and $0.4 \mu\text{M} + 0.1 \mu\text{M}$, respectively; Table 2). The sites at CC1 and SR1 had the highest average N:P values (both at $160 + 240$). There were significant spatial differences in the concentrations of nitrate and phosphate ($p < 0.001$ and $p < 0.001$, respectively) and in the N:P ratio ($p < 0.001$) when comparing the LSS and the HSS. The LSS had higher average concentrations of both nitrate ($12 \mu\text{M} + 6 \mu\text{M}$) and phosphate ($0.3 \mu\text{M} + 0.2 \mu\text{M}$) than the HSS ($9 \mu\text{M} + 3 \mu\text{M}$ and $0.1 \mu\text{M} + 0.08 \mu\text{M}$, respectively). Yet the LSS had lower average N:P ratios ($70 + 60$) than the HSS ($110 + 130$). There was large variability in the N:P ratios within each salinity group, however, as shown by the large standard deviations.

Nitrate concentrations ($p = 0.0063$) and the N:P ratios ($p = 0.016$) were significantly impacted by the tidal stage at which samples were collected. Elevated average nitrate con-

centrations were observed at high tide ($11 \mu\text{M} + 5 \mu\text{M}$) relative to values measured at low and mid tide ($9 \mu\text{M} + 5 \mu\text{M}$ and $10 \mu\text{M} + 5 \mu\text{M}$, respectively). The highest average N:P ratio was observed at mid tide ($110 + 133$) with lower values observed at low tide and high tides ($68 + 62$; $95 + 108$, respectively). But as with the seasonal and spatial average N:P ratios, standard deviations were relatively high when comparing tide classes.

DISSOLVED INORGANIC CARBON

Measurements of inorganic carbon parameters (i.e., pH and carbonate alkalinity) began on July 7, 2021, so data from the spring and early summer are also missing. A significant seasonal trend in pH ($p < 0.001$) was observed with a higher average pH occurring in the summer ($8.4 + 0.3$) than in the autumn ($8.3 + 0.2$). Across all the samples, the average pH was $8.3 + 0.1$. The highest and lowest pH values occurred on Aug 25 ($8.5 + 0.1$) and Oct 27 ($8.1 + 0.2$), respectively (Figure 2D). The pH decreased towards the end of the season, with an October average of $8.20 + 0.06$, compared to a late summer (Aug 25 to Sept 15) average of $8.42 + 0.07$ (Fig. 2D). Based on the analysis of variance, a significant difference in pH between the LSS and HSS was observed ($p = 7.4 \times 10^{-6}$). The LSS had a slightly higher average pH at $8.4 + 0.2$, compared to an average pH of $8.3 + 0.2$ for the HSS locations. The

Spatial and Temporal Variability in Water Quality and Phytoplankton Community Composition

Table 2. Averages of selected water quality measurements with standard deviations in parenthesis, during the entire sampling season. The second line for each site is the range of values during the sampling season. Alkalinity is the carbonate alkalinity and CDOM values represent the absorbance at 412 nm.

Station	Salinity (PSU)	Nitrate (µM)	Phosphate (µM)	pH	Alkalinity (meq/L)	CDOM Absorbance	TChla (µg/L)
AR1	22.0 (2.77)	12.8 (5.57)	0.194 (0.096)	8.35 (0.153)	2.03 (0.488)	0.080 (0.032)	4.12 (2.66)
	17-27	6.33-26.43	0.019-0.350	8.05-8.59	1.29-2.81	0.044-0.156	0.98-13.82
AR2	20.2 (2.80)	14.2 (6.22)	0.287 (0.157)	8.35 (0.181)	1.95 (0.527)	0.101 (0.049)	5.39 (6.01)
	15-26	7.61-31.04	0.083-0.652	8.14-8.75	0.95-2.79	0.045-0.228	0.72-30.24
AR3	12.5 (3.86)	17.7 (8.18)	0.788 (0.862)	8.42 (0.201)	1.82 (0.478)	0.192 (0.076)	5.29 (3.09)
	4-20	5.03-36.24	0.314-4.06	7.89-8.74	1.00-2.47	0.084-0.347	0.96-11.79
CC1	27.0 (1.88)	8.5 (2.70)	0.105 (0.078)	8.31 (0.189)	2.23 (0.437)	0.045 (0.026)	7.18 (6.14)
	24-30	3.97-12.34	0-0.270	7.89-8.57	1.36-2.94	0.025-0.123	2.26-30.05
CH1	23.4 (2.08)	10.6 (3.02)	0.162 (0.042)	8.38 (0.198)	2.09 (0.377)	0.066 (0.033)	5.99 (2.85)
	19-27	5.65-15.94	0.068-0.231	8.05-8.75	1.42-2.69	0.018-0.129	1.54-11.61
CH2	22.6 (2.53)	10.3 (3.09)	0.162 (0.124)	8.26 (0.153)	1.92 (0.770)	0.043 (0.013)	3.05 (1.67)
	17-26	5.09-15.55	0.035-0.453	8.08-8.51	0-2.72	0.021-0.070	0.83-8.21
CH3	24.2 (3.03)	9.0 (3.04)	0.113 (0.097)	8.24 (0.124)	2.18 (0.454)	0.051 (0.026)	4.82 (2.38)
	20-30	4.90-16.04	0-0.394	8.00-8.40	1.50-3.31	0.018-0.125	0.82-9.79
CS1	31.7 (1.76)	7.8 (2.47)	0.136 (0.089)	8.24 (0.166)	2.41 (0.728)	0.038 (0.021)	7.40 (4.56)
	28-34	4.95-13.14	0.042-0.376	7.92-8.46	0.52-3.43	0.019-0.108	2.71-22.19
FB1	33.7 (1.31)	5.6 (2.42)	0.071 (0.076)	8.29 (0.175)	2.46 (0.702)	0.044 (0.038)	5.63 (2.77)
	31-36	1.17-11.14	0-0.231	7.99-8.62	0.66-3.58	0.014-0.140	1.69-14.35
FC1	5.13 (3.75)	11.6 (5.42)	0.304 (0.150)	8.70 (0.326)	1.44 (0.473)	0.132 (0.050)	4.39 (4.75)
	0-13	4.63-26.24	0.103-0.673	8.17-9.47	0.27-2.29	0.040-0.216	0.46-17.51
HC1	21.6 (1.62)	9.6 (2.43)	0.110 (0.071)	8.37 (0.166)	1.96 (0.386)	0.050 (0.021)	4.85 (4.14)
	20-25	4.68-14.01	0.030-0.274	8.09-8.59	1.29-2.67	0.025-0.093	1.48-20.96
HC2	20.9 (1.82)	8.8 (3.95)	0.163 (0.160)	8.32 (0.231)	1.80 (1.026)	0.058 (0.032)	8.73 (7.22)
	18-25	3.23-20.35	0-0.614	7.68-8.67	0-3.06	0.021-0.121	1.87-35.68
JIC1	21.6 (2.28)	10.1 (4.45)	0.199 (0.075)	8.39 (0.215)	2.20 (0.700)	0.080 (0.031)	6.29 (3.67)
	18-26	3.63-21.19	0.044-0.303	8.02-8.83	0.97-3.49	0.029-0.128	1.72-18.82
JIC2	19.1 (2.75)	10.4 (4.40)	0.356 (0.110)	8.36 (0.275)	2.26 (0.460)	0.114 (0.055)	8.12 (5.41)
	14-24	5.56-21.33	0.108-0.504	7.67-8.86	1.47-2.91	0.056-0.232	2.96-28.28
SC1	26.1 (2.05)	8.9 (4.36)	0.113 (0.068)	8.28 (0.336)	2.21 (0.472)	0.048 (0.038)	6.63 (5.01)
	20-28	3.23-19.57	0.022-0.231	7.20-8.85	1.29-2.89	0.021-0.190	2.10-24.56
SC2	25.5 (3.07)	8.4 (3.67)	0.140 (0.082)	8.30 (0.184)	2.29 (0.391)	0.052 (0.027)	5.50 (3.60)
	18-30	1.37-16.73	0.019-0.285	8.02-8.57	1.68-3.16	0.025-0.125	1.48-16.16
SC3	18.7 (8.25)	8.0 (2.96)	0.201 (0.085)	8.34 (0.221)	2.41 (0.626)	0.079 (0.042)	7.31 (9.15)
	2-30	1.70-12.81	0.057-0.331	8.07-8.87	1.06-3.34	0.034-0.175	2.13-49.11
SR1	29.4 (3.92)	7.9 (2.45)	0.106 (0.075)	8.25 (0.163)	2.49 (0.347)	0.079 (0.080)	4.47 (4.04)
	22-35	4.50-13.07	0-0.29	8.08-8.53	1.83-3.11	0.016-0.354	0.85-21.21
WCI	20.9 (3.04)	12.2 (3.61)	0.188 (0.111)	8.37 (0.205)	1.97 (0.539)	0.122 (0.060)	4.52 (2.97)
	15-25	7.02-18.10	0.051-0.467	8.03-8.74	0.31-2.67	0.036-0.250	1.61-12.81
WR1	22.7 (1.25)	9.8 (3.71)	0.097 (0.063)	8.31 (0.168)	2.20 (0.323)	0.047 (0.014)	3.94 (1.95)
	20-25	4.77-20.65	0.015-0.219	8.06-8.62	1.62-2.71	0.026-0.073	1.80-10.27

highest average pH was measured at FC1 (8.7 + 0.3), a LSS, and the lowest average pH was measured at CH3 (8.2 + 0.1), a HSS (Table 2).

No difference in carbonate alkalinity was detected between the seasons ($p = 0.94$). The average carbonate alkalinity during the sampling season was 2.1 meq/L + 0.3 meq/L, with the highest and lowest carbonate alkalinities occurring on October 6 (2.6 meq/L + 0.3 meq/L) and October 20 (1.9

meq/L + 0.4 meq/L), respectively (Figure 2D). However, there was a significant spatial trend in carbonate alkalinity ($p = 7.2 \times 10^{-5}$), with the LSS having a lower average carbonate alkalinity (2.0 meq/L + 0.6 meq/L) than the HSS (2.3 meq/L + 0.5 meq/L). The lowest average carbonate alkalinity was measured at FC1 (1.4 meq/L + 0.5 meq/L), a LSS, and the highest average carbonate alkalinity was measured at FB1 (2.5 meq/L + 0.7 meq/L), a HSS (Table 2).

CHROMOPHORIC DISSOLVED ORGANIC MATTER

Measurements of CDOM were estimated from the absorbance of seawater filtrate at 412 nm. There was no significant seasonal trend in CDOM absorbance ($p = 0.14$), which might be due to the lack of data from the spring and early summer as these measurements only began on the July 7 sampling date. Over the course of the sampling season, the average CDOM absorbance was 0.08 ± 0.02 , with the lowest CDOM absorbance occurring on July 7 (0.05 ± 0.02) and the highest CDOM absorbance values occurring on August 4 and September 1 (0.11 ± 0.05 and 0.11 ± 0.07 , respectively; Figure 2C).

A spatial trend in CDOM absorbance was observed as these values were significantly different between the LSS and the HSS groups ($p < 0.001$). The LSS had a higher average CDOM absorbance (0.10 ± 0.06) than the HSS (0.05 ± 0.03 ; Figure 2C). Of all the sites, AR3, a LSS location, had the highest average CDOM absorbance (0.2 ± 0.08) and CS1, a HSS location, had the lowest average CDOM absorbance (0.04 ± 0.02 ; Table 2). To further investigate the relationship between CDOM absorbance and salinity, linear regressions between these two variables were run on the LSS and HSS data separately. The LSS data had a significant, positive correlation between CDOM and salinity ($R^2 = 0.321$), suggesting that the input of CDOM is more likely coming from upriver of the sites than from downriver (Figure 3). The slope of the regression line of the HSS data ($R^2 = 0.001$) was not significantly different from zero (Figure 3). CDOM absorbance was significantly impacted by the tidal stage at which samples were collected ($p = 0.014$), resulting in a slight gradient pattern with the high-

est CDOM absorbance values measured at low tide (0.09 ± 0.06), the lowest CDOM absorbance being measured at high tide (0.06 ± 0.06) and the CDOM absorbance measured at the mid tide falling in between (0.07 ± 0.06). This trend supports the hypothesis that a significant source of the CDOM is likely located upriver of the sampling sites.

PHYTOPLANKTON BIOMASS

Average TChla concentrations significantly changed during the sampling season ($p < 0.001$), with the highest average TChla being measured in the summer at $7.1 \mu\text{g/L} \pm 5.9 \mu\text{g/L}$, compared to $5.1 \mu\text{g/L} \pm 2.3 \mu\text{g/L}$ in the spring and $4.1 \mu\text{g/L} \pm 2.9 \mu\text{g/L}$ in the autumn. More specifically, TChla increased from April 28 ($3.8 \mu\text{g/L} \pm 1.5 \mu\text{g/L}$) through Aug 11 ($14.2 \mu\text{g/L} \pm 3.8 \mu\text{g/L}$) and then decreased throughout the remainder of the season ($2.8 \mu\text{g/L} \pm 0.9 \mu\text{g/L}$ on Oct 27) with relatively high variability between weeks (Figure 4A). The maximum TChla was observed on August 11 and the minima TChla were observed on October 20 and October 27, with averages of $2.8 \mu\text{g/L} \pm 0.6 \mu\text{g/L}$ and $2.8 \mu\text{g/L} \pm 0.9 \mu\text{g/L}$, respectively. No significant spatial trend in TChla was detected between the LSS and HSS groups ($p = 0.34$). Of the sites, HC2 had the highest average TChla at $8 \mu\text{g/L} \pm 6 \mu\text{g/L}$ and CH2 had the lowest average TChla at $3 \mu\text{g/L} \pm 2 \mu\text{g/L}$, however large standard deviations (Table 2) revealed seasonal variability, as previously mentioned, and tidal variability ($p < 0.001$). When samples were collected at high tide, the average TChla concentration was $4.9 \mu\text{g/L} \pm 3.7 \mu\text{g/L}$, compared to $5.1 \mu\text{g/L} \pm 2.9 \mu\text{g/L}$ at mid tide and $6.8 \mu\text{g/L} \pm 6.1 \mu\text{g/L}$ at low tide. Since samples from multiple sites were not collected on July 28 (6 sites) and August 18 (4 sites), these two weeks were

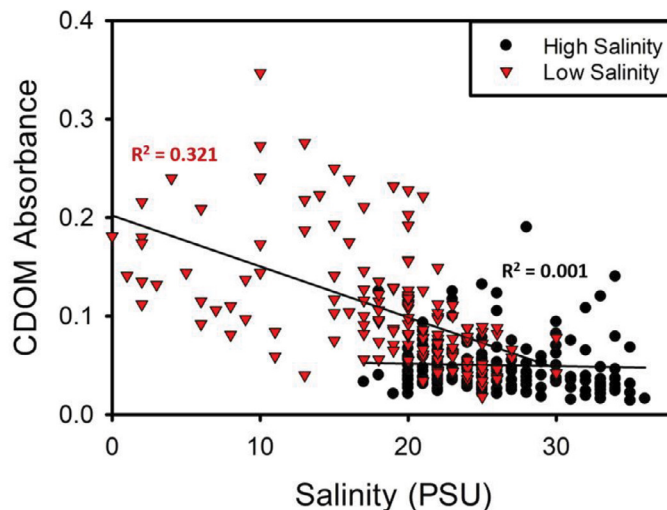


Figure 3. Correlation between salinity and CDOM absorbance at 412 nm. Data were grouped into 'low salinity sites' and 'high salinity sites' as defined in the results and Table 1. R^2 values are from linear regressions run on each group separately.

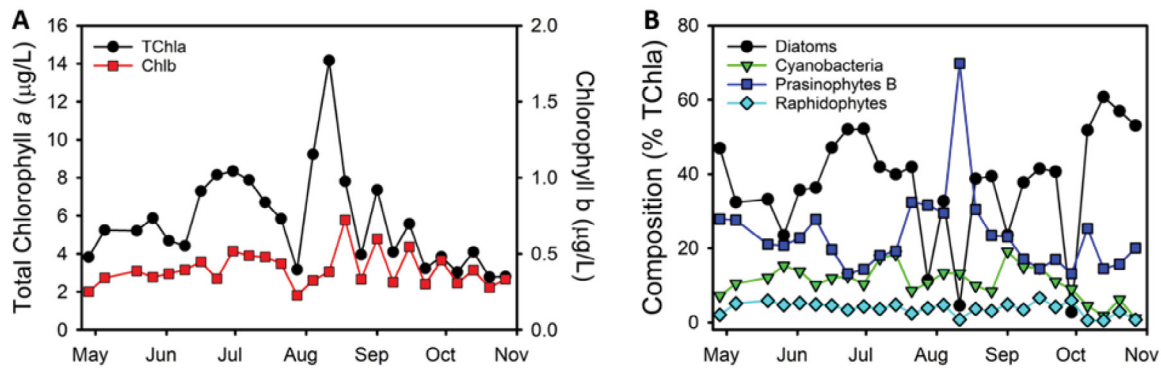


Figure 4. (A) Average total chlorophyll a and chlorophyll b throughout the sampling season. (B) Community composition as the percent of TChla contributed by each algal group, as determined by CHEMTAX analysis

not included in the calculation of site averages of TChla and Chlorophyll *b* (Chlb) to prevent bias.

Chlb was used as a proxy for the biomass of small, flagellated phytoplankton species including chlorophytes, euglenophytes, and prasinophytes (Lewitus et al. 2005). Seasonal differences in Chlb were observed ($p = 0.015$). Chlb concentrations were the lowest in the spring with an average concentration of $0.3 \mu\text{g/L} \pm 0.1 \mu\text{g/L}$ (Figure 4A). In the summer and autumn, Chlb increased to $0.4 \mu\text{g/L} \pm 0.3 \mu\text{g/L}$ and $0.4 \mu\text{g/L} \pm 0.2 \mu\text{g/L}$, respectively (Figure 4A). The lowest concentration of Chlb was measured on July 28 ($0.2 \mu\text{g/L} \pm 0.1 \mu\text{g/L}$), three weeks before the season maximum on August 18 ($0.7 \mu\text{g/L} \pm 0.7 \mu\text{g/L}$). After August 18, Chlb concentration decreased with great variability between weeks during the remainder of the sampling season (similarly to TChla), returning to low concentrations in October ($0.33 \mu\text{g/L} \pm 0.05 \mu\text{g/L}$) (Figure 4A). Of all the sites, the highest and lowest average Chlb concentrations occurred at JIC2 ($0.6 \mu\text{g/L} \pm 0.3 \mu\text{g/L}$) and CH2 ($0.25 \mu\text{g/L} \pm 0.05 \mu\text{g/L}$), respectively. Like TChla, there was no difference between Chlb concentrations in the LSS and HSS groupings ($p = 0.10$), but differences in Chlb were detected between tide class ($p = 1.0 \times 10^{-12}$). The average Chlb was $0.3 \mu\text{g/L} \pm 0.1 \mu\text{g/L}$ at high tide, $0.4 \mu\text{g/L} \pm 0.2 \mu\text{g/L}$ at mid tide and $0.5 \mu\text{g/L} \pm 0.3 \mu\text{g/L}$ at low tide.

PHYTOPLANKTON COMMUNITY COMPOSITION

Overall, the phytoplankton community in the greater Charleston Harbor area was taxonomically diverse. Over half of the approximately 500 samples contained at least seven of the nine algal groups included in the CHEMTAX analysis. Across all samples, diatoms, prasinophytes B, haptophytes and cyanobacteria were the four most abundant algal groups, averaging $38\% \pm 15\%$, $23\% \pm 11\%$, $12\% \pm 9\%$ and $11\% \pm 5\%$ of the community composition, respectively. Raphidophytes, a potentially toxin-producing algal group, contributed an

average of $4\% \pm 2\%$ of the TChla. The highest species diversity occurred on May 26, when 45% of the stations contained all nine algal groups. Species diversity decreased towards the end of the sampling season, as all nine algal groups were not present at any station during October. The greatest diversity occurred at CS1 and SC3, where all nine algal groups were present on 23% of the sampling weeks. The lowest diversity occurred at FB1, FC1, SR1, and WC1, where all nine algal groups were present on less than 8% of the sampling weeks.

Seasonal trends in diatoms ($p = 0.011$), cyanobacteria ($p = 0.0063$), prasinophytes A ($p < 0.001$) and B ($p < 0.001$), haptophytes ($p < 0.001$), and euglenophytes ($p < 0.001$) were observed. Across the seasons, haptophytes were more abundant in the spring (compared to summer and autumn), cyanobacteria and prasinophytes B were more abundant in the summer (compared to spring and autumn) and diatoms, prasinophytes A and euglenophytes were more abundant in the autumn (compared to spring and summer). Patterns in the relative abundance of diatoms and prasinophytes B, the two most abundant groups, and in cyanobacteria and raphidophytes, two potentially toxin-producing groups, were further investigated across all stations. Some dinoflagellates species are also known to produce toxins, however, the average dinoflagellate abundance was low ($< 2\%$ TChla), so this group was not further investigated. Diatoms were the most abundant group for the majority of the season ($40\% \pm 10\%$), except on July 28, August 11, and September 29, when diatoms contributed only $11\% \pm 6\%$, $5\% \pm 2\%$ and $3\% \pm 6\%$ of the TChla biomass, respectively (Figure 4B). The low abundance of diatoms on July 28 and August 11 coincided with an increase in the abundance of the prasinophyte B group that occurred from July 21 to September 1. Before and after those seven weeks, the prasinophytes B taxa contributed $21\% \pm 5\%$ and $17\% \pm 4\%$ of the phytoplankton community, respectively (Figure 4B). However, from July 21 to September

1, this value increased to $34\% \pm 16\%$ (Fig. 4B). Cyanobacteria made up about $12\% \pm 2\%$ of the TChla biomass from April 28 to June 30 (Fig. 4B). However, this value increased to $17.8\% \pm 0.8\%$ of the TChla biomass on July 7 and 14. The cyanobacterial abundance decreased to $11\% \pm 2\%$ of the TChla biomass from July 21 to August 25 (Figure 4B). This decrease occurred simultaneously with an overall increase in prasinophytes B biomass (Figure 4B). As the abundance of prasinophytes B decreased on Sept 8, cyanobacteria became more abundant, averaging $15\% \pm 3\%$ of the community from September 1 to 22. From April 28 to September 29 the abundance of raphidophytes remained relatively constant at only $4\% \pm 1\%$ of the phytoplankton TChla biomass. As SSTs declined near the end of the sampling period (Oct 6 to 27), diatoms became the dominant algal group again, making up $56\% \pm 4\%$ of the community (Figure 4B). During this same time, the prasinophytes B taxa remained at $19\% \pm 5\%$ of the community and cyanobacteria and raphidophytes decreased to approximately $3\% \pm 2\%$ and $1\% \pm 1\%$, respectively (Figure 4B).

Spatial differences, based on the LSS and HSS, were only observed in the prasinophytes A, chlorophytes, and euglenophytes groups ($p = 5.0 \times 10^{-6}$, 4.2×10^{-4} and 4.1×10^{-7} , respectively). The LSS had larger proportions of chlorophytes ($4\% \pm 5\%$) and euglenophytes ($6\% \pm 6\%$) than the HSS, while the HSS had a larger proportion of prasinophytes A ($4\% \pm 7\%$) than the LSS locations. Regardless of salinity grouping, diatoms were, on average, the most abundant at AR1 ($48\% \pm 16\%$ TChla biomass) and the least abundant at CS1 ($28\% \pm 12\%$ TChla biomass) (Table 3). Prasinophytes B were the most abundant at FB1 ($33\% \pm 17\%$ TChla biomass) and the least abundant at CH2 ($13\% \pm 15\%$ TChla biomass). On average, cyanobacteria and raphidophytes were the most abundant at FC1, contributing to $15\% \pm 14\%$ and $7\% \pm 8\%$ of the TChla biomass, respectively. However, the lowest average abundance of cyanobacteria was measured at SC2 ($7\% \pm 8\%$ TChla biomass) and the lowest average abundance of raphidophytes was measured at WC1 ($2\% \pm 3\%$ TChla biomass) (Table 3).

The relative abundances of dinoflagellates, prasinophytes A, prasinophytes B, chlorophytes, and raphidophytes were impacted by the tidal stage at which samples were collected ($p = 0.017$, 0.029 , 0.018 , $p < 0.001$, and $p < 0.001$, respectively), even though these groups, with the exception of prasinophytes B, each contributed to less than 5% of the TChla biomass. Prasinophytes B were more abundant at high tide ($26\% \pm 21\%$) than at mid and low tides. Dinoflagellates and prasinophytes A were more abundant at mid tide ($1\% \pm 1\%$ and $4\% \pm 8\%$, respectively) than at high and low tides. Chlorophytes and raphidophytes were more abundant at low tide (both at $4\% \pm 4\%$) than at high and mid tides.

The phytoplankton community composition was further investigated in the Ashley River (i.e., AR1, AR2, and

AR3) and Shem Creek (i.e., SC1, SC2, SC3). These sites were selected because they form small-scale transects from relatively lower salinity, upriver locations (i.e., AR3 and SC3) to more saline, downriver sites closer to Charleston Harbor (i.e., AR1 and SC1; Figure 1). These sites are also relatively isolated from the input of larger tributaries with minimal mixing of other bodies of water. Phytoplankton community composition data were selected from four dates that covered the span of the sampling season and when samples were collected at the same tidal stage, which happened to be high tide: April 28 (spring), May 26 (late spring), August 11 (summer), and October 20 (autumn). In both the Ashley River and Shem Creek, the greatest community diversity of this subset occurred on May 26, while the lowest diversity occurred on October 20 in the Ashley River and on August 11 in Shem Creek (Figures 5 and 6). A gradient in diatom abundance was observed in the Ashley River on April 28, May 26, and October 20, where the abundance of diatoms increased as the relative distance to the Charleston Harbor decreased. From AR3 to AR1, diatom abundance increased, from 24% to 71% on April 28, from 25% to 47% on May 26, and from 44% to 65% on October 20 (Figures 1, 5A, B, D). In the Ashley River, cyanobacteria were only present at the furthest upriver site, AR3, on May 26, August 11, and October 20, and at AR2 on May 26 and August 11 (Figures 5B, C, and D). Of these four weeks, cyanobacteria were not present at AR1, the Ashley River site closest to the coast (Figures 1 and 5). In Shem Creek, gradients in the community composition along the transect were less noticeable, as the standard deviations in algal group abundance between the Shem Creek sites was 0.2–3.6 times less than that of the Ashley River sites. This may suggest greater mixing or flushing of Shem Creek than the Ashley River, but it is important to note that the presence or absence of gradients in phytoplankton commu-

Table 3. Sample sites where each algal group was the most and least abundant.

Algal Group	Most abundant at	Least abundant at
Diatoms	AR1	CS1
Dinoflagellates	HC2	CS1
Cyanobacteria	FC1	SC2
Prasinophytes A	CC1	AR2
Prasinophytes B	FB1	CH2
Chlorophytes	FC1	SR1
Raphidophytes	FC1	WC1
Haptophytes	FB1	AR1
Euglenophytes	FC1	FB1

Spatial and Temporal Variability in Water Quality and Phytoplankton Community Composition

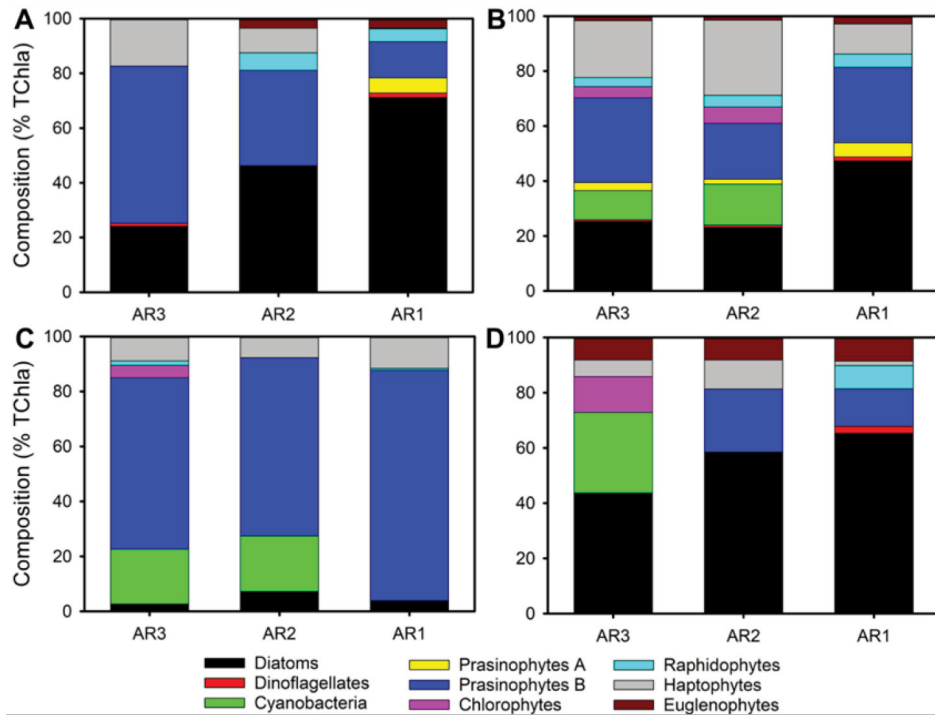


Figure 5. Stacked bar graphs of community composition as the percent of TChla contributed by each algal group from AR3 (furthest upriver), AR2 and AR1 (furthest downriver) on (A) April 28, (B) May 26, (C) August 11, and (D) October 20.

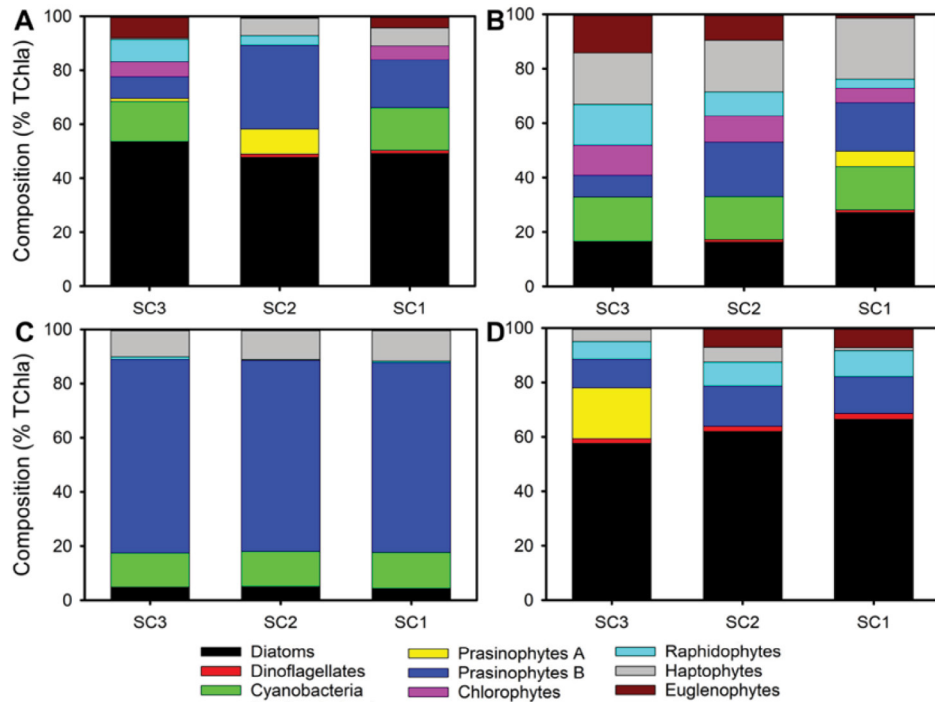


Figure 6. Stacked bar graphs of community composition as the percent of TChla contributed by each algal group from SC3 (furthest upriver), SC2 and SC1 (furthest downriver) on (A) April 28, (B) May 26, (C) August 11, and (D) October 20.

nity composition may be impacted differently by the tidal stage at different locations within the Charleston Harbor.

IMPACT OF IMPERVIOUS SURFACE COVER

It was hypothesized that sites surrounded by a greater proportion of impervious surface cover would be more greatly impacted by stormwater runoff than sites located near more forested, pristine environments, especially after heavy rainfall events. This stormwater runoff is expected to decrease the salinity of local waters while increasing the concentrations of nitrate and phosphate and the relative amount of CDOM. To explore this hypothesis, weeks were selected where the cumulative rainfall from the three days prior to sample collection was greater than 1 inch. These weeks included June 16, June 23, July 28, August 18, September 22, and October 6, although samples for nitrate, phosphate and CDOM absorbance were not collected on June 16 and June 23. Correlations were then run between site impervious surface cover (Table 1) and salinity, nitrate, phosphate and CDOM absorbance. While there was a slight correlation between impervious surface cover and salinity during these weeks ($R^2 = 0.142$), no correlations were observed with the nitrate, phosphate and CDOM data ($R^2 = 0.021, 0.005$ and 0.004 , respectively). The lack of strong correlation between impervious surface cover and these water quality variables may suggest that other metrics (e.g., land use) would be better indicators of where and how urbanization is likely to influence surface and stormwater runoff into the Charleston Harbor.

PRINCIPAL COMPONENT ANALYSIS

The final PCA using the 11 water quality and biological variables included data from only the high and low tide classes (Figure 7). When the mid tide class data were also included, the first two principal components explained less variance (39.1%) than when the mid tide class was omitted (41.6%). An inverse relationship was observed between salinity and nitrate and phosphate concentrations (Figure 7). This result suggests that the source of nitrate and phosphate into Charleston Harbor is likely coming from upriver, as opposed to from the incoming tide. Salinity was also inversely correlated with cyanobacteria and raphidophytes, suggesting that these algal groups are more abundant in fresher waters, further upriver, especially at the FC1 site (Table 3), which generally have higher nitrate and phosphate concentrations (Figure 7). TChl a showed a positive correlation with temperature, indicating that overall phytoplankton biomass increased in the summer (in agreement with the analysis of variance results as well), with cyanobacteria, prasinophytes B, and raphidophytes becoming more abundant (Fig. 7). However, diatoms displayed an inverse relationship with temperature. This pattern was also seen in the community composition data, as diatoms were more abundant in late

June/early July and in October (Figure 4B), but when SSTs were highest (in late July to late August), the abundance of diatoms decreased and the prasinophytes B group became more abundant (Figures 2A and 4B).

OVERALL SEASONAL, SPATIAL AND TIDAL PATTERNS

To better understand the general dynamics of the Charleston Harbor estuary, comparisons were made between seasons (spring, summer, and autumn of 2021), between low and high salinity locations (LSS and HSS), and between tidal stages (low, mid, and high tides). When significant seasonal differences were detected, the spring had the lowest average Chl b concentration ($p = 0.015$) and the highest abundance of haptophytes ($p < 0.001$). In the summer, average SSTs were the warmest ($p < 0.001$), TChl a and Chl b concentrations were the highest ($p < 0.001$ and 0.015 , respectively), and cyanobacteria and prasinophytes B were more abundant ($p = 0.0063$ and $p < 0.001$, respectively), compared to other seasons. The autumn had the lowest TChl a concentrations ($p < 0.001$), similar Chl b concentrations to the summer ($p = 0.015$), and a greater abundance of diatoms, prasinophytes A, and euglenophytes ($p = 0.011, p < 0.001$, and $p < 0.001$,

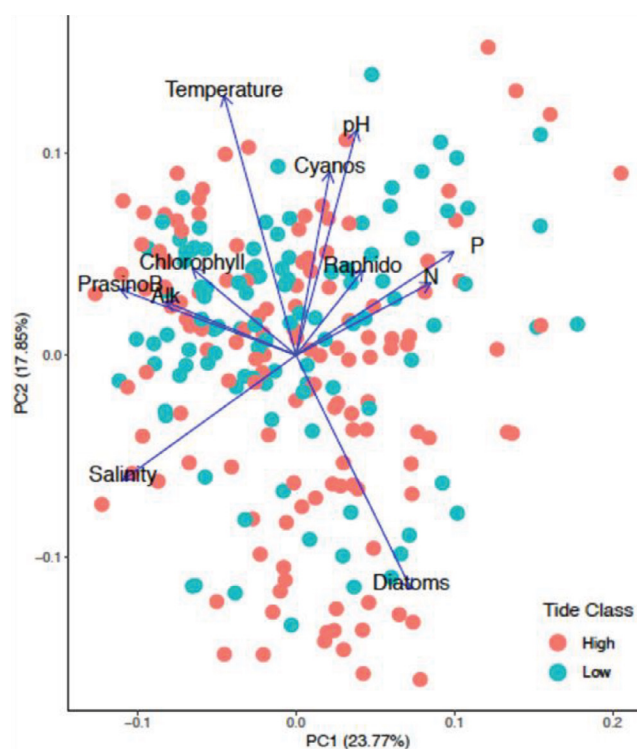


Figure 7. Results from the principal components analysis of eleven variables for data from the “high” (tidal height > 4 ft) and “low” (tidal height < 2 ft) tide classes. Abbreviations: “Cyanos” is cyanobacteria, “Raphido” is raphidophytes, “N” is nitrate, “P” is phosphate, “Alk” is carbonate alkalinity, and “PrasiNoB” is prasinophytes B.

Spatial and Temporal Variability in Water Quality and Phytoplankton Community Composition

Table 4. Summary of seasonal, spatial, and tidal trends in the measured parameters as determined by analysis of variance testing. When significant ($p < 0.05$), the season, salinity grouping or tide class at which the parameter was the highest is listed. “NS” represents no significant difference ($p > 0.05$).

Parameter	Seasonal	Spatial	Tidal
Temperature	Highest in summer	NS	NS
Salinity	NS	Higher at HSS	Highest at high tide
Nitrate	NS	Higher at LSS	Highest at high tide
Phosphate	NS	Higher at LSS	NS
N:P	NS	Higher at HSS	Highest at mid tide
pH	Higher in summer	Higher at LSS	NS
Carbonate alkalinity	NS	Higher at HSS	NS
CDOM absorbance	NS	Higher at LSS	Highest at low tide
TChla	Highest in summer	NS	Highest at low tide
Chlb	Highest in summer	NS	Highest at low tide
Diatoms	Highest in autumn	NS	NS
Dinoflagellates	NS	NS	Highest at mid tide
Cyanobacteria	Highest in summer	NS	NS
Prasinophytes A	Highest in autumn	Higher at HSS	Highest at mid tide
Prasinophytes B	Highest in summer	NS	Highest at high tide
Chlorophytes	NS	Higher at LSS	Highest at low tide
Raphidophytes	NS	NS	Highest at low tide
Haptophytes	Highest in spring	NS	NS
Euglenophytes	Highest in autumn	Higher at LSS	NS

respectively) than in other seasons (Table 4). On average, when significant, the LSS locations were described by lower salinity ($p < 0.001$), higher nitrate and phosphate concentrations ($p < 0.001$ and $p < 0.001$, respectively), lower N:P ($p < 0.001$), higher pH ($p < 0.001$), lower carbonate alkalinity ($p < 0.001$), higher CDOM absorbance ($p < 0.001$) and greater contributions of chlorophytes and euglenophytes ($p < 0.001$ and $p < 0.001$, respectively), compared to the HSS locations, which had a significantly greater abundance of prasinophytes A ($p < 0.001$) (Table 4). When significantly different, samples collected at low tide had on average, the lowest nitrate concentrations and N:P ratios ($p = 0.0063$ and 0.016 , respectively), the highest CDOM absorbance ($p = 0.014$), the highest TChla and Chlb concentrations ($p < 0.001$ and $p < 0.001$, respectively), and the greatest abundances of chlorophytes and raphidophytes ($p < 0.001$ and $p < 0.001$, respectively), with respect to the mid and high tide classes (Table 4).

DISCUSSION

Charleston Harbor is a dynamic estuary with freshwater inputs from the Ashley, Cooper, and Wando Rivers. These rivers bring low salinity, high nutrient and high CDOM waters into the harbor. Nutrient loading and CDOM levels are expected to be impacted by land use and land cover changes, especially in highly urbanized locations like the greater Charleston area. Estuarine systems like the Charleston Harbor will also very likely be impacted by increasing SST and storm flooding events as a result of anthropogenically induced climate change in the coming decades. This is especially concerning as warmer SSTs are expected to increase the abundance, frequency, and toxicity of harmful algal bloom species (Paerl and Huisman 2009; O’Neil et al. 2012). Hence, it is essential to develop a baseline understanding of estuary systems such as the Charleston Harbor, to monitor ecosystem alterations resulting from elevated SST and changes in nutrient inputs. As a result of this study, a baseline collection of water quality parameters and phytoplankton community abundance and

composition was compiled, allowing for short-term seasonal changes in the Charleston Harbor estuary to be observed. A longer time series study of the Charleston Harbor, however, will be needed to determine the significance of temporal variability of water quality parameters on phytoplankton community composition.

The abundance and composition of the phytoplankton community in the Charleston Harbor estuary changed throughout the course of the sampling season, from late spring to early autumn of 2021. Seasonal changes in SST significantly impacted phytoplankton species biodiversity (Figures 5 and 6). The results of the PCA showed a shift in phytoplankton community composition as diatoms were inversely correlated with temperature, while prasinophytes B and cyanobacteria were positively correlated with temperature (Figure 7). Specifically, diatoms were more abundant in late spring and early autumn, while prasinophytes B, and to a lesser extent cyanobacteria, were more abundant in the summer (Figure 4). The observed trend of increased diatom abundance at cooler SST and increased prasinophytes B and cyanobacteria abundance at warmer SST could be related to decreased grazing pressure on the large phytoplankton cells (i.e., diatoms) at cooler temperatures (Cloern 2017). Similarly, the warmer SST in summer can fuel higher growth rates of smaller cells (i.e., prasinophytes and cyanobacteria) compared to diatoms. Accumulation of small cell abundance in summer could suggest that the grazing rates on these small cells were lower than the growth rates (Cloern 2017). The observed seasonal shift in the phytoplankton community composition could have ecosystemwide impacts on carbon cycling and energy transfer to higher trophic levels, especially when considering that diatoms can effectively fuel fish production while small, flagellated cells drive the microbial loop resulting in lower fishery yields (Cloern 2017; Richardson and Jørgensen 1996).

When analyzing the small-scale transect within the Ashley River, it was observed that cyanobacteria were present in the two stations further upstream (AR3 and AR2) and were absent in the furthest downstream station, near the Charleston Harbor (AR1; Figures 1 and 5). The positive correlations observed between cyanobacterial abundance and nitrate and phosphate, concomitant with the inverse correlation with salinity suggests that cyanobacteria are more abundant in the relatively nutrient-rich, low salinity waters of the local rivers than in the higher salinity waters of the Charleston Harbor. Within estuary systems, cyanobacteria abundance and distribution are often limited by high salinity (Moisander et al. 2002; Marino et al. 2006), further supporting this trend.

While seasonal patterns in nutrient concentrations displayed high variability, it was evident that the Charleston Harbor estuary had an excess of nitrate, with respect to phosphate, as N:P ratios were well above the predicted Redfield ratio required for phytoplankton growth (Figure

2B; Table 2). A strong negative correlation between salinity and both nitrate and phosphate suggest that the source(s) of these nutrients are located upstream from the Charleston Harbor and are likely related to river runoff (Figure 7). High N-loading probably reflects the fact that nitrate, unlike phosphate, does not bind to soil particles. Hence, nitrate is more likely to be flushed from exposed soils than phosphate (Burton et al. 1977). This excess of nitrate may have supported the diatom-dominated phytoplankton community that was observed during most of the sampling season, as diatoms are often abundant in high-nitrogen waters (Pinckney et al. 1998; Lomas and Glibert 1999; Carstensen et al. 2015). High N:P ratios and low phosphate concentrations suggest that phosphate may be a limiting macronutrient, potentially controlling the low abundance of cyanobacteria (Figure 4B). For instance, some cyanobacterial species are N-fixers and presumably would have a competitive advantage in low N environments if released from phosphate limitation (Moisander et al. 2002; Pliński et al. 2007).

At present, there exists a paucity of water quality data (e.g., nutrient concentrations) published for the Charleston Harbor estuary, especially within the past decade. However, studies have been conducted near Murrells and North Inlets, SC, and further south in the Skidaway River estuary, Georgia, as well as the St. Johns River estuary and Indian River Lagoon in Florida. These water quality studies included streams, tidal creeks, and estuaries from the 1980s to late 2010s (Tufford et al. 2003; Bittar et al. 2016; Dame et al. 2000; Van Meerssche and Pinckney 2018; Lapointe et al. 2020; Pinckney et al. 2020; Wang and Zhang 2020). The nitrate concentrations measured in the present study ($10 \mu\text{M} \pm 3 \mu\text{M}$) were very comparable to those measured in nearby estuaries, which ranged from 2–38 μM . However, the phosphate concentrations measured in the Charleston Harbor were on the low end of the range measured in other southeast estuaries ($0.2 \mu\text{M} \pm 0.1 \mu\text{M}$ compared to 0.2–3.8 μM ; Tufford et al. 2003; Bittar et al. 2016; Dame et al. 2000; Van Meerssche and Pinckney 2018; Lapointe et al. 2020; Pinckney et al. 2020; Wang and Zhang 2020). A global review of 86 estuarine coastal locations reported median nitrate and phosphate concentrations of 10.4 μM and 0.38 μM , respectively (N:P = 27; Carstensen et al. 2015). The present study in Charleston Harbor observed similar nitrate concentrations, but again lower phosphate concentrations than many other global estuaries, which explains the exceptionally high average N:P ratio observed in the present study (91 ± 43). Such high N:P ratios suggest the possibility of phosphate limitation on phytoplankton growth, with respect to other estuarine ecosystems. It should be noted, however, that our study did not measure total N (e.g., contributions from ammonium N and urea N) and as a result the N:P ratios reported here are actually conservative values relative to the true *in-situ* N:P ratios. It is also possible, however, that high ammonium levels could inhibit nitrate

uptake rates thereby elevating the N:P ratio further (Lomas and Glibert 1999). Future studies should incorporate measurements of ammonium and urea, especially with respect to mounting evidence regarding the prevalence of failing septic tanks leaking nutrients into local waters (e.g., James Island Creek and Shem Creek).

Wetlands and estuaries act as a nursery bed for many aquatic species and evidence is accumulating that they are also important ecosystems for the sequestration of “blue” carbon (Macreadie et al. 2021). Ecosystem models and resource managers will need to assess how shifts in the phytoplankton community, driven by physical and chemical changes, could impact food web dynamics within tidal marsh ecosystems like the Charleston Harbor estuary. For instance, a shift from diatoms to smaller, flagellated photoautotrophs could fuel a microbial-based food web and decrease the trophic transfer of carbon to commercially important species such as shrimp, crabs, oysters, and fish. Interactive effects of elevated SST and elevated N:P ratios could also trigger the increase in some HAB-forming species (Paerl et al. 2007; Peñuelas et al. 2013) and potentially jeopardize the overall ecosystem health of the estuary. Hence, incorporating phytoplankton community structure into ecological models will become increasingly important and will allow resource managers to carefully gauge the threat of HABs and the potential human health risks associated with their presence. On a global scale, the ecological impacts of elevated N:P ratios on natural and managed aquatic ecosystems are highly complex and will vary both spatially and temporally due to hydrodynamic and food web interactions (Peñuelas et al. 2013; Carstensen et al. 2015).

While Charleston Harbor is being significantly impacted by increasing urbanization, it is also currently undergoing dredging to deepen the shipping channel (USACE 2015). This deepening will cause significant changes to the physical structure of Charleston Harbor and could potentially result in longer residence times due to an increase in the volume of the estuary. Phytoplankton and bacteria populations would presumably have more time to assimilate nutrients and metabolize CDOM, respectively, which could lead to enhanced microbial biomass and the potential for oxygen depletion. A reduced flushing rate in Charleston Harbor could also favor the development of mixotrophic species such as some HAB-forming cyanobacteria and dinoflagellate species, especially considering that more frequent, episodic flooding events will increase the delivery of CDOM from local rivers (Figure 3; Valdes-Weaver et al. 2006). To have a better understanding of the Charleston Harbor estuary system, ecosystem models will need to incorporate hydrodynamic alterations to flow patterns caused by the recent deepening of the channel. The data collected from this study will provide a convenient reference point for comparative future studies on hydrography

and phytoplankton diversity, especially in reference to the Charleston Harbor deepening project.

The results of this study provide a baseline dataset of water quality and phytoplankton community composition from late spring to early autumn of 2021 in the Charleston Harbor estuary. While this dataset only included April through October, seasonal, spatial, and tidal impacts were observed. For instance, seasonal changes in SST were linked to a shift from diatoms to picoplanktonic flagellates such as prasinophytes. This estuary was also influenced by the input of nutrient and CDOM-rich riverine waters that supported a cyanobacterial population upriver of the Charleston Harbor, especially at the Filbin Creek site. Anthropogenic and climate change-related impacts on the Charleston Harbor estuarine ecosystem will become more important in the coming decades. Understanding changes in water quality and phytoplankton diversity in the face of environmental variability will be important for resource managers, especially to help inform future decisions regarding food sustainability and ecosystem health in the greater Charleston Harbor region.

ACKNOWLEDGMENTS

We would like to acknowledge Cheryl Carmack, Andrew Wunderley, and all the volunteers with Charleston Waterkeeper (<https://charlestonwaterkeeper.org/>) for their work in the sample and field data collection. Partial support for this research was provided by a NASA EpSCOR R3 grant to G. DiTullio and A. Ali.

The authors would like to acknowledge the time invested and the constructive comments made by two anonymous reviewers that significantly improved the quality of the manuscript.

REFERENCES

- Anderson DM, Gilbert PM, Burkholder, JM. Harmful algal blooms and eutrophication: Nutrient sources, composition, and consequences. *Estuaries*. 2002; 25: 704–726.
- Bittar TB, Berger SA, Birsa LM, Walters TL, Thompson ME, Spencer RGM, Mann EL, Stubbins A, Frischer ME, Brandes JA. Seasonal dynamics of dissolved, particulate, and microbial components of a tidal saltmarsh-dominated estuary under contrasting levels of freshwater discharge. *Estuarine, Coastal, and Shelf Science*. 2016; 182A: 72–85. doi:10.1016/j.ecss.2016.08.046.
- Carmichael WW. Health effects of toxin-producing cyanobacteria: “The CyanoHABs.” *Human and Ecological Risk Assessment: An International Journal*. 2001; 7(5): 1393–1407. doi: 10.1080/20018091095087.
- Carstensen J, Klais R, Cloern JE. Phytoplankton blooms in estuarine and coastal waters: Seasonal patterns and key

- species. *Estuarine, Coastal, and Shelf Science*. 2015; 162 (5): 98–109. doi: 10.1016/j.ecss.2015.05.005.
- Cloern JE, Jassby AD. Complex seasonal patterns of primary producers at the land-sea interface. *Ecology Letters*. 2008; 11: 1294–1303. doi: 10.1111/j.1461-0248.2008.01244.
- Cloern JE. Why large cells dominate estuarine phytoplankton. *Limnology and Oceanography*. 2017; 63(S1). doi:10.1002/lno.10749.
- Chin T, Beecraft L, Wetz MS. Phytoplankton biomass and community composition in three Texas estuaries differing in freshwater inflow regime. *Estuarine, Coastal, and Shelf Science*. 2022; 277: 108059. doi: 10.1016/j.ecss.2022.108059.
- Dame R, Alber M, Allen D, Mallin M, Montague C, Lewitus A, Chalmers A, Gardner R, Gilman C, Kjerfve B et al. Estuaries of the south Atlantic coast of North America: Their geographical signatures. *Estuaries*. 2000; 23 (6): 793–819.
- DiTullio GR, Geesey MR. Photosynthetic pigments in marine algae and bacteria, In G. Bitton eds. *The encyclopedia of environmental microbiology*. New York: John Wiley & Sons; 2002. p. 2453–2470. doi:10.1002/0471263397.env185.
- Fernandes LF, Hubbard KA, Richlen ML, Smith J, Bates SS, Ehrman J, Leger C, Mafra Jr. LL, Kulis D, Quilliam M et al. Diversity and toxicity of the diatom *Pseudo-nitzschia Peragallo* in the Gulf of Maine, Northwestern Atlantic Ocean. *Deep-Sea Research Part II: Topical Studies in Oceanography*. 2013;103:139–162. doi: 10.1016/j.dsr2.2013.06.022.
- Freeman LA, Corbett DR, Fitzgerald, AM, Lemley DA, Quigg A, Steppe CN. Impacts of urbanization and development on estuarine ecosystems and water quality. *Estuaries and Coasts*. 2019;42:1821–1838.
- Groffman PM, Boulware NJ, Zipperer WC, Pouyat RV, Band LE, Colosimo MF. Soil nitrogen cycle processes in urban riparian zones. *Environmental Science and Technology*. 2002;36(21):4547–4552. doi: 10.1021/es020649z.
- Gurley LN, Kolb KR. Land cover basin characteristics rasters for South Carolina StreamStats. 2021 U.S. Geological Survey data release. doi:10.5066/P9LYEMJU.
- Higgins HW, Wright SW, Schlüter L. Quantitative interpretation of chemotaxonomic pigment data. In: Roy S, Llewellyn CA, Egeland ES, Johnson G, editors. *Phytoplankton pigments: Characterization, chemotaxonomy, and applications in oceanography*. Cambridge (UK): Cambridge University Press; 2011. p. 257–313.
- Kirchman, DL, Cottrel, MT, DiTullio, GR. Shaping of bacterial community composition and diversity by phytoplankton and salinity in the Delaware Estuary, USA. *Aquatic Microbial Ecology*. 2017;78:93–106. doi: 10.3354/ame01805.
- Lapointe BE, Herren LW, Brewton RA, Alderman PK. Nutrient over-enrichment and light limitation of seagrass communities in the Indian River Lagoon, an urbanized subtropical estuary. *Science of the Total Environment*. 2020;699: 134068. doi: 10.1016/j.scitotenv.2019.134068.
- Lee SY, Dunn RJK, Young RA, Connolly RM, Dale PER, Dehayr R, Lemckert CJ, McKinnon S, Powell B, Teasdale PR, Welsh DT. Impact of urbanization on coastal wetland structure and function. *Australian Ecology*. 2006;31:149–163. doi:10.1111/j.1442-9993.2006.01581.
- Lewitus AJ, White DL, Tymowski RG, Mackey ME, Hymel SN, Noble PA. Adapting the CHEMTAX method for assessing phytoplankton taxonomic composition in Southeastern U.S. estuaries. *Estuaries*. 2005; 28:160–172. doi:10.1007/BF027327.
- Lomas MW, and Gilbert PM. Temperature regulation of nitrate uptake: A novel hypothesis about nitrate uptake and reduction in cool-water diatoms. *Limnology and Oceanography*. 1999;44, 556–572.
- Mackey MD, Mackey DJ, Higgins HW, Wright SW. CHEMTAX- program for estimating class abundances from chemical markers: Application to HPLC measurements of phytoplankton. *Marine Ecology Progress Series*. 1996; 144: 265–283.
- Mallin MA, Pearl HW, Rudek J. Seasonal phytoplankton composition, productivity and biomass in the Neuse River estuary, North Carolina. *Estuarine, Coastal, and Shelf Science*. 1991;32(6):609.623. doi: 10.1016/0272-7714(91)90078-P.
- Morris JT, Renken KA. Past, present, and future nuisance flooding on the Charleston peninsula. *PLoS ONE*. 2020;15(9): e0238770. doi: 10.1371/journal.pone.0238770.
- Paerl HW, Valdes-Weaver LM, Joyner AR, Winkelmann V. Phytoplankton indicators of ecological change in the eutrophying Pamlico Sound System, North Carolina. *Ecological Applications*. 2007; 17(sp5). doi:10.1890/05-0840.1.
- Paerl HW, Huisman J. Climate change: A catalyst for global expansion of harmful cyanobacterial blooms. *Environmental Microbiology Reports*. 2009; 1(1): 27–37. doi: 10.1111/j.1758-2229.2008.00004.
- Parsons TR, Maita Y, Lalli CM. *A manual of chemical and biological methods for seawater analysis*. Pergamon Press; 1984.
- Peñuelas J, Poulter B, Sardans J, Ciais P, van der Velde M, Bopp L, Boucher O, Godderis Y, Hinsinger P, Llusia J, et al. Human-induced nitrogen–phosphorus imbalances alter natural and managed ecosystems across the globe. *Nature Communications*. 2013;4:2934.
- Pinckney JL, Paerl HW, Harrington MB, Howe KE. Annual cycles of phytoplankton community-structure and bloom dynamics in the Neuse River Estuary, North Carolina. *Marine Biology*. 1998;131:371–381. Applications 17, S88-S101.
- Pinckney JL, Knotts ER, Kibler KJ, Smith EM. Nutrient breakpoints for estuarine phytoplankton communities. *Limnology and Oceanography*. 2020;65:2999–3016. doi: 10.1002/lno.11570.
- Pliński M, Mazur-Marzec H, Józwiak T, Kobos J. The potential causes of cyanobacterial blooms in Baltic Sea

Spatial and Temporal Variability in Water Quality and Phytoplankton Community Composition

- estuaries. *Oceanological and Hydrobiological Studies*. 2007;36(1):134–137. doi:10.2478/v10009-007-0001-x.
- Redfield AC. On the proportions of organic derivatives in sea water and their relation to the composition of plankton. *James Johnstone memorial volume*. 1934;176–192. w22222.
- Reed ML, DiTullio GR, Kacenas SE, Greenfield DI. Effects of nitrogen and dissolved organic carbon on microplankton abundances in four coastal South Carolina (USA) systems. *Aquatic Microbial Ecology*. 2015;76:1–14.
- Riekenberg J, Bargu S, Twilley R. Phytoplankton community shifts and harmful algae presence in a diversion influenced estuary. *Estuaries and Coasts*. 2015;38:2213–2226.
- Rothenberger MB, Burkholder JAM, Wentworth TR. Use of long-term data and multivariate ordination techniques to identify environmental factors governing estuarine phytoplankton species dynamics. *Limnology and Oceanography*. 2009;54(6):2107–2127. doi:10.4319/lo.2009.54.6.2107.
- Sarazin G, Michard G, Prevot F. A rapid and accurate spectroscopic method for alkalinity measurements in sea water samples. *Water Research*. 1999;33(1):290–294
- Schlesinger WH, Bernhardt ES. *Biogeochemistry: An analysis of global change*. Elsevier. 2013;(3):688.
- Statham PJ. Nutrients in estuaries—an overview and the potential impacts of climate change. *Science Total Environment*. 2012;434: 213–237. doi: 10.1016/j.scitotenv.2011.09.088.
- Tufford DL, Samarghitan CL, McKellar Jr. HN, Porter DE, Hussey JR. Impacts of urbanization on nutrient concentrations in small southeastern coastal streams. *Journal of the American Water Resources Association*. 2003;39(2):301–312.
- USACE. Charleston harbor post 45 draft integrated feasibility report/environmental impact statement. U.S. Army Corps of Engineers, Charleston District; 2015.
- Valdes-Weaver LM, Piehler MF, Pinckney JL, Howe KE, Rossignol K, Paerl HW. Long-term temporal and spatial trends in phytoplankton biomass and class-level taxonomic composition in the hydrologically variable neuse-Pamlico Estuarine Continuum, North Carolina. U.S.A. *Limnology and Oceanography*. 2006;51(3):1410–1420. doi:10.4319/lo.2006.51.3.1410.
- Van Meerssche E, Pinckney JL. Nutrient loading impacts on estuarine phytoplankton size and community composition: Community-based indicators of eutrophication. *Estuaries and Coasts*. 2018;42:504–512. doi: 10.1007/s12237-018-0470-z.
- Verma A, Barua A, Ruvindy R, Savela H, Ajani PA, Murray SA. The genetic basis of toxin biosynthesis in dinoflagellates. *Microorganisms*. 2019;7(8):222. doi: 10.3390/microorganisms7080222.
- Wang J, Zhang Z. Phytoplankton, dissolved oxygen, and nutrient patterns along a eutrophic river-estuary continuum: Observation and modeling. *Journal of Environmental Management*. 2020;261:110233. doi: 10.1016/j.jenvman.2020.110233.
- Xu C, Liu W. The spatiotemporal characteristics and interactions between urban expansion and tidal flat dynamics: A case study of three highly urbanized coastal counties in the Southeastern United States. *Earth*. 2022;3(2):557–576. doi: 10.3390/earth3020033.